

Models, methods and performance when estimating the compression ratio based on the cylinder pressure

Marcus Klein and Lars Eriksson

Vehicular Systems, Linköpings Universitet, SWEDEN

ABSTRACT

Four methods for compression ratio estimation of an engine from cylinder pressure traces are described and evaluated for both motored and fired cycles. The first three methods rely upon a model of polytropic compression for the cylinder pressure, and it is shown that they give a good estimate of the compression ratio for simulated cycles at low compression ratios. For high compression ratios, this simple model lack the information about heat transfer and the model error causes the estimates to become biased. Therefore a fourth method is introduced where heat transfer and crevice effects are modeled, together with a commonly used heat release model for firing cycles. This method is able to estimate the compression ratio more accurately at low as well as high compression ratios.

INTRODUCTION

A newly developed engine, which can continuously change the compression ratio, has been developed at SAAB Automobile AB. The ability to change the compression ratio opens up new opportunities to increase the efficiency of SI engines by down sizing and super charging. But if the compression ratio gets stuck at too high ratios, the risk of engine destruction by heavy knock increases rapidly. If the compression ratio gets stuck at too low ratios, we get an unnecessary low efficiency, and therefore an unnecessary high fuel consumption. It is therefore vital to monitor and diagnose the continuously changing compression ratio on-line. Due to geometrical uncertainties, a spread of the compression ratio among the different cylinders is inherent [1], and since it is hard to measure the compression ratio directly, estimation is required. The questions asked here are related to: 1) accuracy, 2) convergence speed and 3) over all convergence. The accuracy is of course limited due to measurement noise and model uncertainties.

The approach investigated is to use cylinder pressure to estimate the compression ratio. A desirable property of the estimator is that it must be able to cope with the unknown offset introduced by the charge amplifier, changing

thermodynamic conditions, and possibly also the unknown phasing of the pressure trace in relation to the crank angle revolution.

Two models of cylinder pressure with different complexity levels, a polytropic model and a single-zone zero-dimensional heat release model [2] are used. To estimate the parameters in the cylinder pressure models, three different optimization algorithms minimizing the prediction error are utilized, namely:

1. *A linear subproblem approach*, where groups of the parameters are estimated one at a time and the predictor function is rewritten to be linear for the group of estimated parameters. Thus we can use linear regression at every substep for estimating the particular group of parameters.
2. *A variable projection method* [3], where one iteration consists of two substeps: The first substep estimates the parameters that are linear in the predictor function, holding the nonlinear constant. The second substep is to perform a line search in the direction of the negative gradient at the parameters found from substep one. This method classifies as a separable least squares method.
3. *Levenberg-Marquardt method*, i.e. a Gauss-Newton method, where we here use numerical approximations of the gradient and the hessian.

Based on these models, four different methods are developed and used for compression ratio estimation for both motored and fired cycles.

THE SVC ENGINE

The principle of the SVC (Saab Variable Compression) engine is shown in Figure 1. By tilting the mono-head the compression ratio can be continuously varied between 8 and 14. The geometric data for the SVC engine are given in Appendix A.

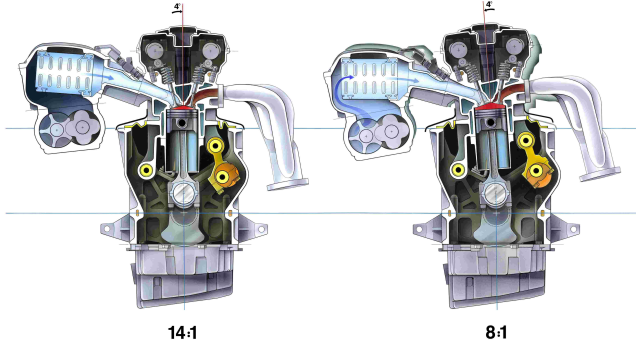


Figure 1: Schematic of engine with variable compression. ©SAAB Automobile AB

SVC volume function

The cylinder volume sweep for the SVC is different in appearance compared to the standard volume function, $V_d(\theta) = \frac{\pi B^2 a}{4} (\frac{l}{a} + 1 - \cos \theta - \sqrt{(\frac{l}{a})^2 - \sin^2 \theta})$, since the geometry of the crank in relation to the cylinder changes when the cylinder head is tilted. This motivates the study done in [4] which is only briefly recapitulated here. The cylinder volume $V^{SVC}(r_c, \theta)$ for the SVC engine can be written as

$$V^{SVC}(r_c, \theta) = V_c^{SVC}(r_c) + V_d(\theta - \theta_{corr}(r_c)) \quad (1)$$

where $\theta - \theta_{corr}(r_c) = \theta'$ is the corrected crank angle, r_c is the compression ratio and V_c^{SVC} is the clearance volume for the SVC engine. The dependence of the correction term $\theta_{corr}(r_c)$ for r_c is shown in Figure 2. Simulations show that the relative error between the SVC volume function and the standard volume function is less than 0.6 % for every crank angle.

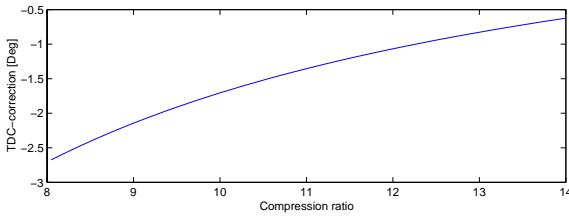


Figure 2: Top dead center correction as function of compression ratio.

CYLINDER PRESSURE MODELING

Two models are used for describing the cylinder pressure trace and they are referred to as the polytropic model and the standard model.

Polytropic model A simple but efficient model is the polytropic compression model,

$$p(\theta)V(\theta)^n = C \quad (2)$$

where p is the cylinder pressure, $V(\theta)$ is the volume function, n is the polytropic coefficient and C is a cycle-to-cycle dependent constant. The model is valid during the compression phase of the engine cycle, but not during combustion. This means that for a firing cycle only data between inlet valve closing (IVC) and start of combustion (SOC) will be used, but for motored cycles all data between inlet valve closing (IVC) and exhaust valve opening (EVO) is utilized.

Standard model The article by Gatowski et.al. [2] develops, tests and applies the heat release analysis procedure used here. It maintains simplicity while still including the effects of heat transfer and crevice flows. The model has been widely used and the phenomena that it takes into account are well known [5]. Therefore, only a short summary of the model is given here. The pressure differential dp can be written as

$$dp = \frac{\delta Q_{ch} - \frac{\gamma}{\gamma-1} p dV - \delta Q_{ht}}{\frac{1}{\gamma-1} V + \frac{V_{cr}}{T_w} \left(\frac{T}{\gamma-1} - \frac{1}{b} \ln \left(\frac{\gamma-1}{\gamma'-1} \right) + T' \right)} \quad (3)$$

This is an ordinary differential equation that easily can be solved numerically if a heat-release trace, δQ_{ch} is provided. For this purpose the well-known Wiebe function is used in its differentiated form.

The Wiebe function has the following form

$$x_b(\theta) = 1 - e^{-a \left(\frac{\theta - \theta_0}{\Delta \theta} \right)^{m+1}} \quad (4)$$

and its differentiated form is

$$\frac{d}{d\theta} x_b(\theta) = \frac{a(m+1)}{\Delta \theta} \left(\frac{\theta - \theta_0}{\Delta \theta} \right)^m e^{-a \left(\frac{\theta - \theta_0}{\Delta \theta} \right)^{m+1}}$$

where x_b is the mass fraction burned, θ_0 is the start of the combustion, $\Delta \theta$ is the total combustion duration, and a and m are adjustable parameters. This model is valid between inlet valve closing (IVC) and exhaust valve opening (EVO).

ESTIMATION METHODS

Cylinder pressure referencing

Piezoelectric pressure transducers are used for measuring the in-cylinder pressure, which will cause a drift in the pressure trace. This drift is assumed to be constant during one engine cycle, and can be estimated with various methods [6]. Here the measured pressure trace $p_m(\theta)$ will be referenced by comparing it to the intake manifold pressure p_{man} just before inlet valve closing (IVC), for several samples of p_{man} . Due to standing waves in the intake runners at certain operating points, the referencing might prove to be insufficient, so a second pressure referencing will be made for method 3 and 4.

Method 1

The first method estimates the polytropic exponent n , the compression ratio r_c and the constant C in the polytropic model. The method iteratively solves two problems, one to determine the polytropic exponent n , and the other to determine the compression ratio r_c . By using the polytropic model (2)

$$p(\theta)(V_c(r_c) + V_d(\theta'))^n = C \quad (5)$$

the compression ratio r_c can be estimated by iteratively estimating the clearance volume V_c (i.e. r_c) and the polytropic coefficient n .

Substep 1: The polytropic coefficient n is assumed to be known and the clearance volume is estimated by rewriting (5). This yields a least square subproblem which is linear in the parameters C_1 and V_c according to

$$V_d(\theta') = C_1 p(\theta)^{-1/n} - V_c(r_c) \quad (6)$$

where $C_1 = C^{1/n}$ and V_c are the parameters to be estimated.

Substep 2: The polytropic coefficient n is then estimated using the estimate of V_c from substep 1. Applying logarithms on (5) yields

$$\ln p(\theta) = C_2 - n \ln(V_d(\theta') + V_c(r_c)) \quad (7)$$

which is linear in the parameters n and $C_2 = \ln C$. The linear parameters are estimated and we return to substep 1. This procedure is repeated until convergence.

Method 2

The second method also uses the polytropic compression model (2), together with a variable projection algorithm. A nonlinear least squares problem $\min_x \|r(x)\|^2$ is separable if the parameter vector x can be partitioned such that $x = (y \ z)^T$

$$\min_y \|r(y, z)\|_2 \quad (8)$$

is easy to solve. If $r(y, z)$ is linear in y , $r(y, z)$ can be rewritten as

$$r(y, z) = F(z)y - g(z) \quad (9)$$

For a given z , this is minimized by

$$y(z) = [F^T(z)F(z)]^{-1}F(z)g(z) = F^\dagger(z)g(z) \quad (10)$$

using linear regression. The original problem can then be rewritten as

$$\min_z \|r(y, z)\|_2 = \min_z \|g(z) - F(z)y(z)\|_2 \quad (11)$$

and

$$\begin{aligned} r(y, z) &= g(z) - F(z)y(z) = g(z) - F(z)F^\dagger(z)g(z) \\ &= (I - P_{F(z)})g(z) \end{aligned} \quad (12)$$

where $P_{F(z)}$ is the orthogonal *projection* onto the range of $F(z)$, thus the name variable projection method.

The polytropic model in (5) is rewritten as

$$\ln p(\theta) = C_2 - n \ln(V_d(\theta') + V_c) \quad (13)$$

which is the same equation as (7). This equation is linear in the parameters $C_2 = \ln C$ and n and nonlinear in V_c and applies to the form given in (9). A computationally efficient algorithm is described in [3] and is summarized for our application in Appendix B. For this application the method converges within four iterations.

Method 3

The third method uses the polytropic compression equation (2) as methods 1 and 2 did, but a pressure sensor model is added according to

$$p(\theta) = p_m(\theta) + \Delta p \quad (14)$$

in order to make the pressure referencing better. The crank angle phasing $\Delta\theta$ of the volume and pressure traces is also included in the polytropic model, which then can be written as

$$p(\theta) = p_m(\theta' + \Delta\theta) + \Delta p = C \cdot (V_d(\theta' + \Delta\theta) + V_c)^{-n} \quad (15)$$

Based on Equation 15 the following nonlinear least squares problem is formulated

$$\min_x \|r\|_2 = \min_x \sum_{i=1}^N (p_m(\theta_i) + \Delta p - C \cdot (V_d(\theta_i + \Delta\theta) + V_c)^{-n})^2 \quad (16)$$

A Levenberg–Marquardt method, see e.g. [7], is used to solve this nonlinear least squares problem. The problem has good numerical properties, the Levenberg–Marquardt method has second order local convergence and for this application the method converges within ten iterations.

Method 4

The fourth method uses the single zone model (3) from [2] which includes heat transfer and crevice effects, and it will be used to improve the estimation accuracy. The free parameters which were also used in [8] are summarized in Appendix C. Due to the complexity of this model, the sublinear approach and variable projection approach are not suitable for optimization, and therefore only the Levenberg–Marquardt method is used. The increased complexity of the model also causes identifiability problems for the estimated crevice volume V_{cr} and the estimated compression volume V_c , which appear to be strongly correlated. Therefore during estimation the crevice volume is set constant. As in method 3, the residual between modeled and measured cylinder pressure is formed (compare (16)) and minimized in a least squares sense using the same Levenberg–Marquardt method as before. This approach has earlier

been successfully applied in [9] for motoring cycles, but here a heat-release model is included to cope with firing cycles.

Summary of methods

The following table shows the relation between the different methods.

	Polytropic Model	Standard Model
Opt alg 1	Method 1	
Opt alg 2	Method 2	
Opt alg 3	Method 3	Method 4

For firing cycles, methods 1, 2 and 3 will only use cylinder pressure data between inlet valve closing (IVC) and start of combustion (SOC), in contrast to method 4 which will use data from the entire closed part of the engine cycle, i.e. between inlet valve closing (IVC) and exhaust valve opening (EVO). For motoring cycles, all data during the closed part of the cycle is utilized by all methods.

SIMULATION RESULTS

Since the true values of the compression ratios of the engine are unknown, simulations of the cylinder pressure trace are necessary to perform and use for evaluating the four proposed methods. Only then can it be determined whether the estimates are unbiased or not.

Cylinder pressure simulations were made using the standard model (3) with representative parameters (Appendix C). Sixty different realizations of Gaussian noise with mean value 0 and standard deviation 2 kPa were then added to the simulated cylinder pressures for firing and motored cycles respectively. The following sections shows the typical behavior of the estimation methods for a representative cycle at a high compression ratio $r_c = 13$, where the effects of heat transfer are more likely to show due to the higher pressure and temperature in the cylinder. Residuals for all methods are found in figures 4 to 10 and figures 12 and 13 show a summary of all estimations for motored and fired cycles respectively. In the summary section, statistics of the performance for the four methods are summarized for both firing and motoring cycles.

Method 1

Method 1 converges in a few iterations for almost all simulated cylinder pressures, both for firing and motored cycles. Figure 3 shows the simulated cylinder pressure at compression ratio $r_c = 13$, during the compression and expansion phase of a motored cycle. Using the simulated cylinder pressure an estimation of the parameters is made, and from these a residual from the simulated and estimated cylinder pressure can be found. In Figure 4, the residual corresponding to the cylinder pressure in Figure 3

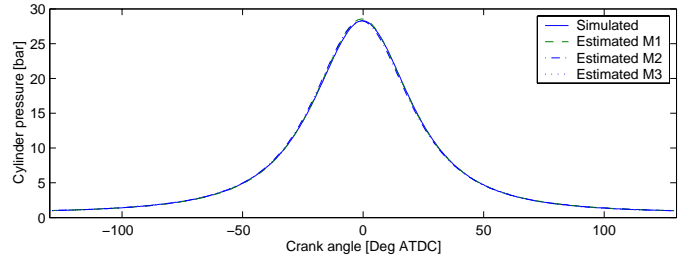


Figure 3: Simulated cylinder pressure for a motored cycle at $r_c = 13$.

is shown. At the beginning of the compression phase and

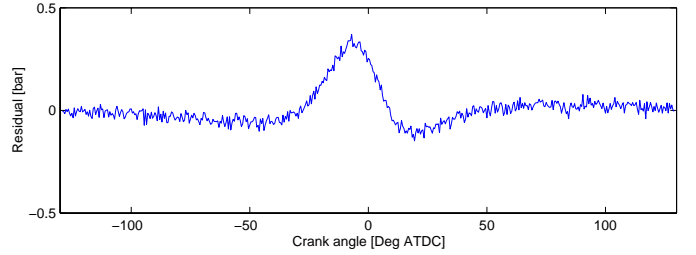


Figure 4: Difference between estimated and simulated cylinder pressure using method 1, for a motored cycle at $r_c = 13$.

at the end of the expansion, the model and estimation method works satisfactory, but not in between where most of the heat transfer occurs. This model inaccuracy is partly covered by allowing the polytropic exponent to be small. Convergence can not be guaranteed for this method, since the predictor function is rewritten in every substep. If the same predictor function could be used at every substep, the problem would be bilinear in the parameters and converge linearly [3]. If the stopping criteria is based upon the convergence of the estimated parameter values, the situation from figure 5 can occur, where the estimated parameters move away from the true parameter values. On the other

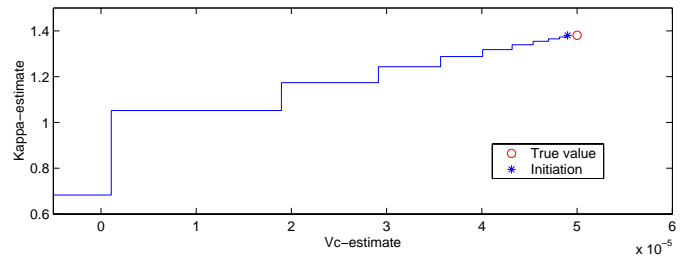


Figure 5: The estimated values of V_c and n at every substep for method 1 when diverging.

hand, if the stopping criteria is based upon the value of the loss function, defined as the sum of squared residuals, the algorithm will stop in time, but the estimate will most likely be biased. Using the loss function, the method stops

in one iteration, i.e. two substeps.

Methods 2 and 3

Methods 2 and 3 show the same lack of model accuracy as method 1, although the estimated compression ratio becomes nearly unbiased. Looking at the residuals in Figure 6 (method 2) and Figure 7 (method 3), stemming from the simulated cylinder pressure in Figure 3, we see the same systematic deviation between the estimated model and the simulation as was seen for the previous methods.

But when lowering the compression ratio the model be-

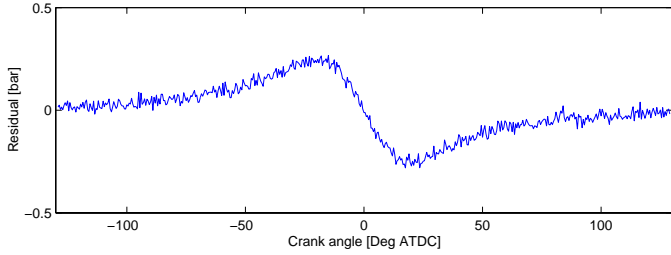


Figure 6: Difference between estimated and simulated cylinder pressure using method 2, for a motored cycle at $r_c = 13$.

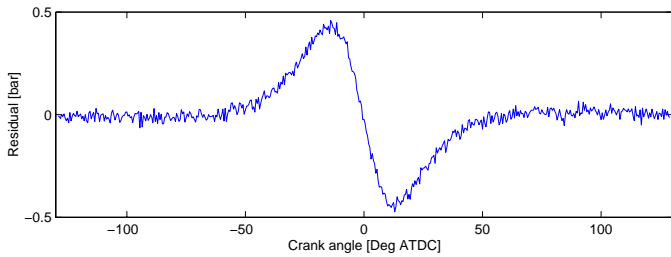


Figure 7: Difference between estimated and simulated cylinder pressure using method 3, for a motored cycle at $r_c = 13$.

comes more accurate, the residual in Figure 8 does not show the same systematic deviation as the residual in Figure 7 did. This is due to that the heat transfer and crevice effects are smaller, which is due to the lower pressure and temperature rendering from the lower compression ratio. The systematic deviation for the residuals are expected since the crevice flow and heat transfer are not considered here and it stresses that these phenomena must be taken into account when a better estimate is desired. Therefore in method 4 a model for the heat transfer and crevice flow is included, together with a heat release model.

Method 4

Reasonable enough, the more complex method also shows the best ability to adjust to the simulated cylinder pressure

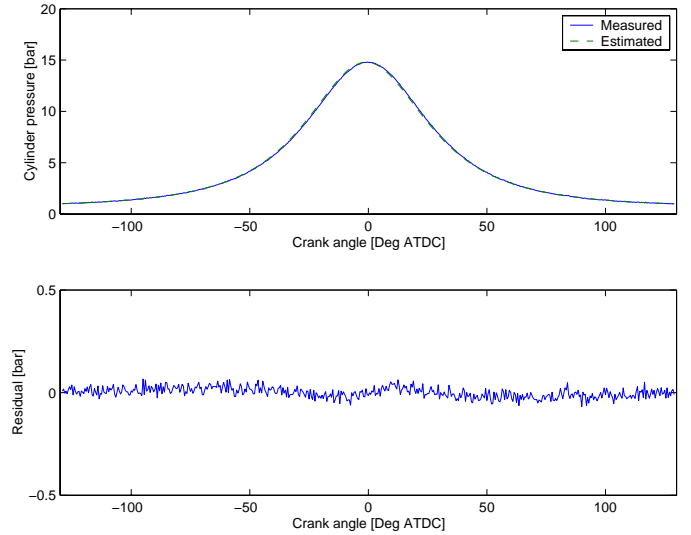


Figure 8: Difference between estimated and simulated cylinder pressure using method 3, for a motored cycle at $r_c = 8$.

and explain the physical phenomena taking place in the cylinder. The residual between simulated and estimated cylinder pressure for a motored cycle at $r_c = 13$ is shown in Figure 9. The residual looks like white noise, suggest-

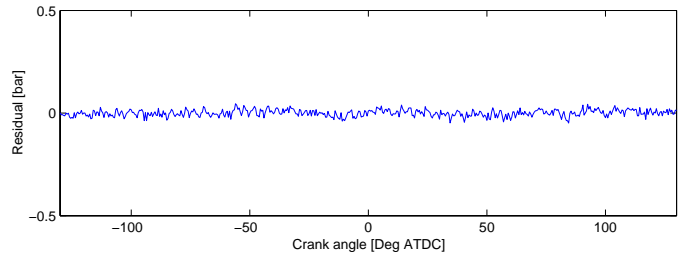


Figure 9: Difference between estimated and simulated cylinder pressure using method 4, for a motored cycle at $r_c = 13$.

ing that the estimation method can explain the data fully. This is also the case for firing cycles, see Figure 10 where the simulated and estimated cylinder pressure is shown together with the residual. As mentioned in Estimation methods, the strong correlation between the crevice volume V_{cr} and the compression volume V_c , shown in figure 11, makes the estimated compression ratio become biased if the crevice volume is also estimated. Therefore the crevice volume is held constant during the estimations.

Summary

Comparing the residuals from all methods, it is obvious that method 4 can explain the data most accurately. This suggests that the estimation of the compression ratio becomes best for method 4, which is also shown in Figure 12

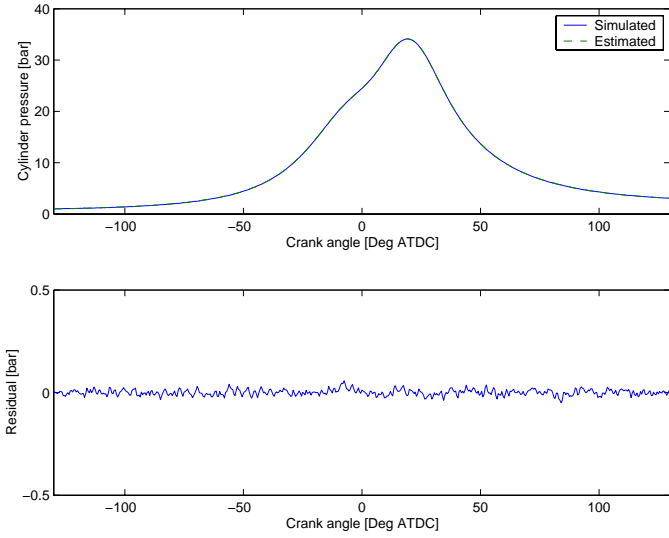


Figure 10: Difference between estimated and simulated cylinder pressure using method 4, for a fired cycle at $r_c = 13$.

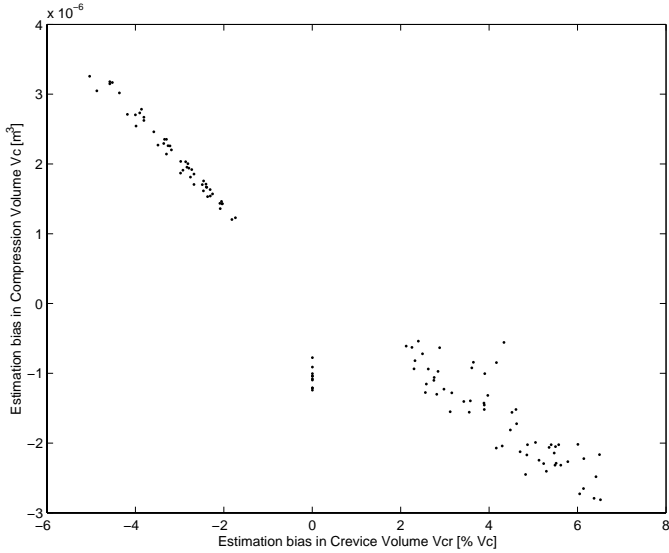


Figure 11: Dependence of estimation bias in crevice volume V_{cr} and estimation bias in clearance volume V_c .

for motored cycles, where the mean and 95% confidence interval of the estimated compression ratio is shown for all four methods. The 95% confidence interval is computed by assuming that the model is correct and that the estimation error asymptotically converges to a Gaussian distribution. In the figure the real compression ratios are the integer values 8 til 13 and for convenience, method 1 is moved to the left, method 2 is moved a little to the left (and to the right of method 1), method 3 is moved a little to the right and method 4 is to the right of method 3. The estimates should be as close to the horizontal lines as possible. Method 1 over estimates the compression ratio, a systematic discrepancy that becomes larger for higher compression ratios.

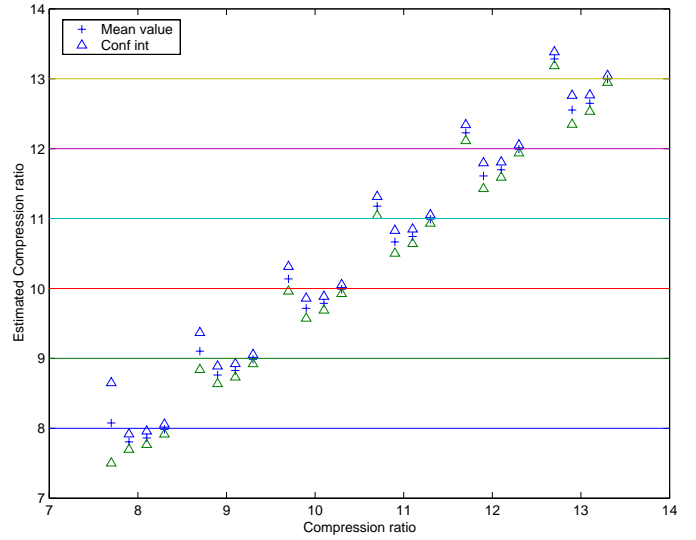


Figure 12: Mean and 95% confidence interval of the estimated compression ratio for motored cycles using the four methods, compared to the real compression ratio.

As mentioned before, this is allowed by letting the polytropic coefficient become small. Methods 2 and 3 on the other hand under estimates the compression ratio, and this systematic fault increases with the compression ratio, in the same way as for method 1. Methods 2 and 3 give approximately the same estimates and 95 % confidence intervals, suggesting that the more time efficient one should be used. Method 4 is able to estimate the compression ratio correctly, due to the higher flexibility of the model.

For firing cycles the same effect as for the motoring cycles appears and is even more pronounced as shown in Figure 13. Table 1 summarizes the standard deviation and the maximum relative error of the estimated compression ratio for 60 cycles respectively. The maximum error is smallest for method 4 both for firing and motoring cycles. The standard deviation is small for all methods. Surpris-

Method	Type	Std dev	Max rel error
1	Fired	0.0319	0.0326
	Motored	0.0175	0.0258
2	Fired	0.1236	0.0396
	Motored	0.0243	0.0202
3	Fired	0.1284	0.0251
	Motored	0.0112	0.0144
4	Fired	0.0620	0.0112
	Motored	0.0156	0.0029

Table 1 Table showing the standard deviation and maximal relative error of the estimated compression ratio r_c , for every method using simulated firing and motoring cycles respectively.

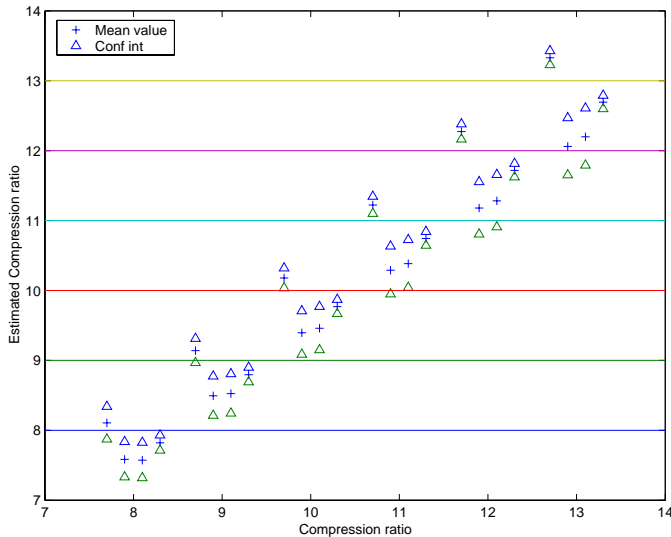


Figure 13: Mean and 95% confidence interval of the estimated compression ratio for fired cycles using the four methods, compared to the real compression ratio.

ingly, the compression ratio estimation is biased even for method 4 for firing cycles.

To conclude, the first three methods rely upon the assumption of a polytropic compression and expansion and it is shown that this is sufficient to get a rough estimate of the compression ratio, especially for low compression ratios and by letting the polytropic exponent to become small. But for higher r_c s it is important to take the heat transfer into account, and then only method 4 is accurate enough. It is interesting to note that for diagnostic purposes, all four methods will be able to detect when the compression ratio gets stuck at a too high or too low level.

The time complexity for the four methods is quite diverse, and is summarized in table 2. The simulations were made using Matlab 6.1 on a SunBlade 100, which has a 64-bit 500 Mhz processor.

Method	Time	# Iter	# Parameters
1	11.2 ms	1	3
2	23 ms	3	3
3	145 ms	5	5
4	$2 * 10^5$ ms	9	12

Table 2 Table showing the mean time and mean number of iterations in completing one cycle, together with the number of parameters for all methods.

FUTURE WORK

The compression volume V_c and the crevice volume V_{cr} are difficult to decouple using the current standard model

from [2]. This issue will be looked into more detail, and will perhaps require a new model for the crevice effect.

CONCLUSIONS

During driving, all methods are able to detect if the compression ratio is stuck at a too high or at a too low level. This is sufficient both for safety reasons, where the compression ratio can be too high and engine knock is the consequence, and for fuel economic reasons, where a too low compression ratio will lead to higher fuel consumption. The four estimation methods all give good estimations for low compression ratios on simulated data. But for high compression ratios, the heat transfer has to be accounted for and therefore the more complex method 4 gives a better estimation than the simpler and more time efficient methods 1, 2 and 3. Method 2 is preferable to method 3 due to its faster convergence.

ACKNOWLEDGEMENTS

This work was financially funded by the Swedish Agency for Innovation Systems (VINNOVA).

REFERENCES

- [1] Charles A. Amann. Cylinder-pressure measurement and its use in engine research. *SAE Technical Paper 852067*, 1985.
- [2] J. A. Gatowski, E. N. Balles, K. M. Chun, F. E. Nelson, J. A. Ekchian, and J. B. Heywood. Heat release analysis of engine pressure data. *SAE Technical Paper 841359*, 1984.
- [3] Å. Björck. *Numerical Methods for Least Squares Problems*. Siam, 1996.
- [4] Y. Nilsson. Cylinder volume function for svc engines. Technical Report LiTH-R-2408, Department of Electrical Engineering, Linköping University, SE-581 83 Linköping, Sweden, 2001.
- [5] J. B. Heywood. *Internal Combustion Engine Fundamentals*. McGraw-Hill series in mechanical engineering. McGraw-Hill, 1988.
- [6] Andrew L. Randolph. Methods of processing cylinder-pressure transducer signals to maximize data accuracy. *SAE Technical Paper 900170*, 1990.
- [7] Philip E. Gill, Walter Murray, and Margaret H. Wright. *Practical Optimization*. Academic Press, 1981.
- [8] Marcus Klein, Lars Eriksson, and Ylva Nilsson. Compression estimation from simulated and measured cylinder pressure. *Electronic Engine Control*, (SAE Technical Paper no.2002-01-0843), 2002.

[9] Lars Eriksson. Requirements for and a systematic method for identifying heat-release model parameters. *Modeling of SI and Diesel Engines*, SP-1330(SAE Technical Paper no.980626):19–30, 1998.

A SVC – GEOMETRIC DATA

Geometric data for the crank and piston movement are given in the following table.

Property	Abbrev.	Value	Unit
Bore	B	68	[mm]
Stroke	S	88	[mm]
Crank radius	$a = \frac{S}{2}$	44	[mm]
Connecting rod	l	158	[mm]
No. of cylinders		5	[-]
Displacement volume	V_d	1598	[cm ³]

B VARIABLE PROJECTION ALGORITHM

An computationally efficient algorithm is described in [3] and is summarized here. Let $x_k = (y_k, z_k)$ be the current approximation.

1. Solve the linear subproblem

$$\min_{\delta y_k} \|F(z_k)\delta y_k - (g(z_k) - F(z_k)y_k)\|_2 \quad (17)$$

and set $x_{k+1/2} = (y_k + \delta y_k, z_k)$.

2. Compute the Gauss-Newton direction p_k at $x_{k+1/2}$, i.e. solve

$$\min_{p_k} \|C(x_{k+1/2})p_k + r(y_{k+1/2}, z_k)\|_2 \quad (18)$$

where $C(x_{k+1/2}) = (F(z_k), r_z(y_{k+1/2}, z_k))$ is the Jacobian matrix.

3. Set $x_{k+1} = x_{k+1/2} + \alpha_k p_k$ and return to step 1.

The polytropic model in (5) is rewritten as

$$\ln p(\theta) = C_2 - n \ln(V_d(\theta') + V_c) \quad (19)$$

This equation is linear in the parameters $C_2 = \ln C$ and n and nonlinear in V_c and applies to the form given in (9). With the notation from the algorithm above, the parameters are $x = (C_2 \ n \ V_c)^T$, where $y = (C_2 \ n)^T$ and $z = V_c$. The measurement vector is formed as $g = -\ln p$ and the regression vector as $F = [-I \ \ln(V_c + V_d(\theta'))]$.

C PARAMETERS IN SINGLE ZONE MODEL

The parameters used in the single zone model (3) are summarized in the following table:

Par.	Description	Value
γ_{300}	constant ratio of specific heat [-]	1.3
b	slope for ratio of specific heat [K^{-1}]	$-8 \cdot 10^{-5}$
C_1	heat transfer parameter [-]	1
C_2	heat transfer parameter [-]	0.5
θ_0	crank angle phasing [deg ATDC]	-0.5
θ_{ig}	ignition angle [deg ATDC]	-15
θ_d	flame development angle [deg ATDC]	20
θ_b	rapid burn angle [deg ATDC]	20
V_c	clearance volume [cm ³]	26.6–45.7
V_{cr}	single aggregate crevice volume [cm ³]	0.16
p_0	bias in pressure measurements [kPa]	10
T_w	mean wall temperature [K]	400
T_{ivc}	mean charge temperature at IVC [K]	330
p_{ivc}	cylinder pressure at IVC [kPa]	100
Q_{in}	released energy from combustion [J]	500